Carbohydrate Polymers 118 (2015) 257–265

Contents lists available at ScienceDirect

Carbohydrate Polymers

journal homepage: www.elsevier.com/locate/carbpol

Digestibility prediction of cooked plantain flour as a function of water content and temperature

A. Giraldo Toro[a,b], O. Gibert[a], J. Ricci[a], D. Dufour[a,c,d], C. Mestres[a], P. Bohuon[b,*]

[a] Centre de Coopération Internationale en Recherche Agronomique pour le Développement (CIRAD), UMR QualiSud, Food Process Engineering Research Unit, 34398 Montpellier, France
[b] Montpellier SupAgro, UMR QualiSud, Food Process Engineering Research Unit, 1101 avenue Agropolis, CS 24501, 34093 Montpellier cedex 5, France
[c] International Center for Tropical Agriculture (CIAT), Km 17 Recta Cali-Palmira, AA 6713 Cali, Colombia
[d] Centre de Coopération Internationale en Recherche Agronomique pour le Développement (CIRAD), UMR QUALISUD, Food Process Engineering Research Unit, AA 6713 Cali, Colombia

ARTICLE INFO

Article history:
Received 11 July 2014
Received in revised form 30 October 2014
Accepted 3 November 2014
Available online 20 November 2014

Keywords:
Starch
Phase transitions
Gelatinization
Nutritional quality
Modelling

ABSTRACT

The effect of temperature (T = 55–120 °C) and water content (X_1 = 1.4–2.0 kg kg^{-1} dry basis) on the gelatinization and digestibility of plantain flour (Dominico Harton genotype) were investigated. The degree of plantain starch gelatinization (α) was measured by DSC and modelled as a function of T and X_1, using the Weibull model. Rapidly digestible starch (*RDS*) and resistant starch (*RS*) fractions were evaluated for different α values. An appropriate dimensionless variable was introduced to the analyzed and modelled *RDS* and *RS* as a function of α. Starch gelatinization begins at a temperature above 59.6 ± 0.5 °C and α is strongly dependent on T in non-limiting water conditions. The combined effects of T and X_1 on the *RDS* and *RS* can be explained by α. We demonstrate that various heat treatments and water contents lead to the same α, with the same *RDS* and *RS* values.

1. Introduction

Banana (*Musa* sp.) is a staple food for millions of people worldwide, particularly in sub-tropical countries, with global production estimated at 139.1 MT in 2012 (FaoStat, 2013). The Cavendish dessert banana is by far the most widely produced cultivar (49%). It is predominantly grown in Asia. Cooking bananas (22% of world production) are largely grown in Asia and Africa, while other dessert banana cultivars (14.6%) are cultivated in Asia and Latin America. The plantain group (14.4%), is most common in Africa and Latin America (Lescot, 2013). Most cooking banana varieties require cooking (boiling, roasting or frying) before they can be eaten.

Banana is a major source of macro-elements and contains resistant starch, dietary fibre, rapidly digestible starch, and slowly digestible starch. Native banana starch is also known for its high level of resistant starch, which remains unhydrolyzed after 120 min by α-amylase with a procedure similar to the *in vivo* digestion (Bello-Perez, Agama-Acevedo, Gibert, & Dufour, 2012; Englyst, Kingman, & Cummings, 1992; Zhang & Hamaker, 2012). Englyst and Cummings (1986) reported that a fraction of starch resists α-amylase in green banana and plantain: 53.6% and 66.7%, respectively. Menezes et al. (2010) thus highlighted the potential of unripe banana flours and starches as functional ingredients that present high *in vitro* fermentability. This is due to the high content of unavailable carbohydrates (resistant starch and/or dietary fibre), which, in turn, do not produce a high increase in the postprandial glycaemic response in healthy volunteers (Miao, Zhang, Mu, & Jiang, 2010). Faisant et al. (1995) observed intact starch granules in ileal samples of healthy individuals after ingestion of unripe bananas. The resistant starch fraction of banana flour seems to be higher at the green ripe stage of maturity (Tribess et al., 2009).

Starch susceptibility to enzyme digestion varies depending on the original plant source of the starch. In addition, it is affected by processing, especially starch thermo-hydric history and storage conditions in comparison with raw, unprocessed flour. The physical state of the starch ingested has a major impact on its digestibility, which is closely linked to the processing techniques (thermal processing, such as extrusion cooking, autoclaving, puffing, roasting, baking, frying) (Singh, Dartois, & Kaur, 2010).

Bahado-Singh, Wheatley, Ahmad, Morrison, and Asemota (2006) studied the Glycaemic Index (GI) values for fourteen common Caribbean foods that were carbohydrate-rich and processed

* Corresponding author at: Montpellier SupAgro, UMR QualiSud, 1101 av. Agropolis, B.P. 5098, 34093 Montpellier cedex 5, France. Tel.: +33 4678740 81; fax: +33 4676144 44.
E-mail address: philippe.bohuon@supagro.inra.fr (P. Bohuon).

http://dx.doi.org/10.1016/j.carbpol.2014.11.016
0144-8617/

Abbreviations

a_α	Constant parameter for scale parameter of the Weibull distribution (Eq. (3))
a_Y	Constant parameter for Y response (Eq. (6))
DSC	Differential scanning calorimetry
ΔH_e	Whole variation of enthalpy (kJ kg^{-1} db starch)
ΔH_r	Specific residual variations of enthalpy (kJ kg^{-1} db starch)
G	First endotherm of gelatinization
G_{20}	Glucose hydrolysis at 20 min
G_{120}	Glucose hydrolysis at 120 min
GI	Glycaemic index
M1	Starch fusion peak
RDS	Rapidly digestible starch (kg per 100 kg of dry starch)
RDS^*	Dimensionless rapidly digestible starch
RDS_α	Rapidly digestible starch for α value (kg per 100 kg of dry starch)
RS	Resistant starch (kg per 100 kg of dry starch)
RS^*	Dimensionless resistant starch
RS_α	Resistant starch for α value (kg per 100 kg of dry starch)
T	Temperature (°C)
T_g	Effective glass transition temperature (°C)
TEG	Terminal extent of starch gelatinization
TS	Total starch content (kg per 100 kg of dry starch)
u_δ	Uncertainty of identified parameter δ (at a 95% confidence interval)
ν_1	Water volume fraction (m^3 m^{-3})
X_1	Water content (kg kg^{-1} dry basis db flour)
Y^*	Dimensionless fraction of RDS^* or RS^* (Eq. (6))

Greek symbols

α	Degree of plantain starch gelatinization
β	Shape parameter of the Weibull distribution
γ	Scale parameter of the Weibull distribution (°C)
θ	Location parameter of the Weibull distribution (°C)

using ten healthy subjects. Green banana and green plantain were found to have the lowest GI, reducing the incidence of postprandial spikes in blood glucose levels. Foods processed by boiling and frying were found to have the lowest GI. The greatest increase in the digestibility of plantain flour was observed with autoclaving at 121 °C for 60 min (Niba, 2003).

During cooking with water, the starch undergoes glass transition followed by gelatinization and/or melting transition, depending on the water content (Donovan, 1979; Lelièvre & Liu, 1994; Slade & Levine, 1988). These transitions in turn induce the swelling of granules, leaching of molecular components from the granules, and eventually disruption of the granules. A consequence of crystalline structure loss is an increase in starch digestion (Miao et al., 2010). The starch gelatinization can be estimated by various techniques, such as microscopy, X-ray diffractometry, Differential Scanning Calorimetry (DSC), and many chemical techniques. DSC in particular makes it possible to detect heat flow changes associated to both first-order (gelatinization and melting) and second-order (effective glass transition) transitions (Biliaderis, Maurice, & Vose, 1980; Donovan, 1979; Slade & Levine, 1988). A state diagram model of starch–water mixtures can be established to predict the extent of starch gelatinization/melting. For instance, few starch state diagrams have been established using either the Flory–Huggins equation (van der Sman & Meinders, 2011), or the empirical equation (Briffaz, Mestres, Matencio, Pons, & Dornier, 2013; Kaletunç & Breslauer, 1996). This model could be used as a monitoring tool to control and optimize the cooking process (Briffaz, Bohuon, Méot, Dornier, & Mestres, 2014a) with different targets in terms of texture (Briffaz et al., 2014b) and digestibility. Due to a limited water content (Briffaz et al., 2013) or an insufficient heating temperature (Parada & Aguilera, 2009), a fraction of starch can remain ungelatinized, which leads to significant changes in the starch's functional quality, *e.g.* nutritional (Holm, Lundquist, Björck, Eliasson, & Asp, 1988), An incomplete swelling of starch granule will induce a partial increase in starch susceptibility to enzyme breakdown. Thus, the extent of disruption caused by heat and moisture will directly impact the ease and extent of enzymatic hydrolysis of cooked starch as earlier reviewed (Wang & Copeland, 2013). For raw cooking banana with a water content that ranges between 1.1 and 2.0 kg kg^{-1} db (dry basis) (Gibert et al., 2009), water content is not limiting (Gibert et al., 2010).

Given the potential health benefits of cooked banana products, linked to cooking conditions, this study set out to generate a quantitative relationship between the degree of starch gelatinization (α) measured by DSC and digestibility using an *in vitro* technique. A state diagram of plantain flour could be a powerful tool for developing food processing methods that modify starch resistance to digestion in order to optimize its nutritional quality and enhance its physiological benefits.

2. Materials and methods

2.1. Material

One bunch of Dominico Harton plantain cooking bananas (AAB *Musa* sp.), grown in a non-extensive farming system, was harvested at optimal green stage of maturity on a farm in Puerto Tejada (state of Cauca, Colombia). The second hand of the bunch was always selected to minimize variability. The cooking bananas from the second hand of the bunch were peeled and the pulp was cut into thin slices, oven dried at 40 °C overnight, ground into a fine powder using a laboratory grinder with a 100 μm opening screen grid, prior to flour storage at 4 °C in an airtight plastic bag for further analysis. For starch preparation, freshly cut pieces of pulp, randomly sampled from the second hand of the bunch, were suspended in distilled water and crushed in a 4 L capacity Waring blender (New Hartford, CT). The slurry was filtered through a 100 mesh sieve, washed three times and decanted. After removal of the dark top layer, the starch was centrifuged three times (17,700 × *g* per 10 min). The isolated starch was oven-dried at 40 °C for 48 h, carefully ground in a mortar, and stored at 4 °C in airtight plastic bags for further analysis.

2.2. Methods

2.2.1. Total starch content and free glucose

Total starch content (*TS*) was estimated after hydrolysis by incubation with Termamyl 120 L heat-thermostable α-amylase enzyme (Novo Nordisk, Copenhagen, Denmark) and then with amyloglucosidase (Sigma, St. Louis, MO, USA). The total released glucose was measured by enzymatic colorimetry at 510 nm after reaction with glucose oxidase (GOD, Sigma, St. Louis, MO, USA) and peroxidase (POD, Sigma, St. Louis, MO, USA) enzymes (Holm, Björck, Drews, & Asp, 1986). Free glucose was estimated separately after the extraction of plantain flour using sulphuric acid (5 mM) and the GOD-POD enzymatic system.

2.2.2. Amylose content

The amylose content of plantain starch as a percentage (kg of amylose per 100 kg db starch) was determined in duplicate by Differential Scanning Calorimetry (DSC) using a Perkin Elmer DSC 7

device (Perkin-Elmer, Norwalk, VA, USA) as described by Mestres, Matencio, Pons, Yajid, and Fliedel (1996).

2.2.3. Granulometry

The plantain starch granule size distribution was estimated in triplicate using the Fraunhofer approximation considering opaque particles by laser diffraction using a Malvern mastersizer 3000 (Malvern Instruments Ltd., Worcestershire, UK).

2.2.4. Density

The density of dried flour was estimated using the pycnometric method as per Colonna and Mercier (1985) and the water volume fraction (ν_1) was calculated according to Donovan (1979).

2.2.5. Thermal properties and effective glass transition temperature

The thermal transitions associated with starch gelatinization were determined by the variation of enthalpy (ΔH_e in kJ kg^{-1} db starch) by DSC. The measurements were carried out at a water content (noted X_1) adjusted to 1.4 and 2.0 kg kg^{-1} db and with a heating scan from 25 to 140 °C at a 10 °C min^{-1} rate using sealed stainless steel pans as described by Gibert et al. (2010). X_1 = 1.4 kg kg^{-1} db corresponds to the raw Dominico Harton plantain water content (Gibert et al., 2009) and X_1 = 2.0 kg kg^{-1} db flour corresponds to the maximum water content after cooking Dominico Harton plantain. The temperature of the effective glass transition temperature (T_g) was determined according to Slade and Levine (1988) using the same DSC device. The samples were subjected to partial scans at intermediate temperatures (55, 60, 65, 70 or 75 °C) at 10 °C min^{-1}. Immediately after reaching targeted temperatures, samples were quench-cooled to 25 °C and immediately rescanned to 140 °C at a 10 °C min^{-1} rate. The temperature of the effective T_g was located comparing thermograms obtained after both intermediate heating and complete heating scans.

2.2.6. X-ray diffraction

Diffractometry X-ray diffraction (triplicate) was performed on native plantain flour after adjusting the water content to 90% relative humidity for 20 days under partial vacuum in the presence of a saturated barium chloride solution. The samples (20 mg) were then sealed between two tape foils to prevent any significant change in water content during the measurement. The diffraction diagrams were recorded using a Bruker (Karlsruhe, Germany) D8 Discover spectrometer in accordance with Pérez et al. (2011).

2.2.7. Degree of starch gelatinization

Plantain-water mixtures were introduced in sealed stainless steel pans and heated for 10 min at various temperatures T (55, 60, 65, 70, 75, 80, 90, 100, and 120 °C) and various X_1 using the same DSC device. After being cooled down to 25 °C and held for 1 min, samples were reheated from 25 to 140 °C at a rate of 10 °C min^{-1} to measure the specific residual variations of enthalpy (ΔH_r). To calculate thermal transitions, let us consider "starch gelatinization" as the sum of the thermal transitions (G, M1). The plantain starch gelatinization, noted α, for any water content-temperature combination (X_1, T) is defined by Eq. (1):

$$\alpha = \frac{\Delta H_e - \Delta H_r}{\Delta H_e} \quad (1)$$

where ΔH_e is the whole enthalpy change of plantain starch and ΔH_r corresponds to the specific residual variations of enthalpy. The starch gelatinization was described in terms of the Weibull cumulative model. When plotted against water content X_1, the starch gelatinization was expressed as a function of temperature T providing 3 parameters, as follows:

$$\alpha = 1 - \exp\left[-\left(\frac{T-\theta}{\gamma(X_1)}\right)^{\beta}\right] \quad \text{for } T > \theta \quad (2a)$$

$$\alpha = 0 \quad \text{for } T \le \theta \quad (2b)$$

with $\gamma(X_1) > 0$, $\beta > 0$ and θ as the three parameters of the distribution; β is the shape parameter assumed to be independent of the water content (Van Boekel, 2002), θ is the location parameter of the distribution independent of X_1 and $\gamma(X_1)$ is the scale parameter assuming that it is inversely proportional to the X_1 value, as follows:

$$\gamma = \frac{a_\alpha}{X_1} \quad (3)$$

where a_α is a constant parameter. According to the Weibullian model, the traditional first-order kinetics is a special case of Eq. (2a), where $\beta = 1$.

2.2.8. Degree of starch gelatinization in a test cell

Plantain flour/water samples were prepared by mixing plantain flour with deionized water to reach targeted water contents X_1, in the 1.4–2.0 kg kg^{-1} db range and kept for equilibrium under partial vacuum conditions in the presence of thymol salts to avoid any bacterial or fungal development. Flour/water mixture samples were introduced into a test cell at room temperature. Flour/water mixture samples were heated in a hermetically sealed test cell (10 mL of samples) that was custom-designed in stainless steel as described previously by Jiménez et al. (2010). To achieve the desired temperatures in the 55–120 °C range, a 5 L oil bath (Model CC2, Huber, Offenburg, Germany) was used. The cooking conditions applied in the test cell were defined in order to obtain an equivalent extent of starch gelatinization as per DSC. After each thermal treatment (analyses were conducted in triplicate), the test cell was immediately cooled in an ice-water bath. The flour paste was then removed from the test cell and weighed into stainless steel capsules prior to the DSC measurement. The DSC heating process was performed from 25 °C to 140 °C at a rate of 10 °C min^{-1}. The remaining amount of flour paste in the test cell was the used to measure the starch *in vitro* digestibility.

2.2.9. Starch digestibility

The rapidly digestible (*RDS*) and slowly digestible (*SDS*) fractions were measured in triplicate using a standardized procedure as per Englyst, Veenstra, and Hudson (1996) with slight modifications. The resistant starch (*RS*) was calculated taking into account the *TS* plantain flour value, with *RS* = *TS* − (*RDS* + *SDS*). After thermal treatment, an amount of flour paste (500 mg of starch on db) was removed from the cooking device and introduced in a 50 mL polypropylene centrifuge tube with a screw cap. After the addition of 50 mg of guar gum and 10 mL of pepsin solution (Sigma P7000-25g, St. Louis, MO, USA) at 5 g L^{-1} in 0.01 mol HCl L^{-1} pH 2, the dispersion was homogenized for 1 min using an ultraturrax (Model T18 basic, IKA-Werke, Staufen, Germany). A mixture of enzymes was prepared on a daily basis by mixing 20 ml of deionized water with 3 g of pancreatin for 10 min using a horizontal shaker (100 strokes min^{-1}) prior to centrifugation at 3415 rpm for 10 min at 20 °C. A 15 mL volume of the supernatant was collected and mixed with 0.9 mL of an invertase solution (10 mg mL^{-1}) and 0.6 mL of an amyloglucosidase solution (AMG 400L type LP, Novo Nordisk Copenhagen). After the addition of 5 mL of a sodium acetate buffer (0.5 M pH 6 at 37 °C) to reach a pH of 5.2, 5 mL of the mixture of enzymes was then added. The centrifuge tube was immediately capped and mixed gently horizontally in a water bath at 37 °C. A continuous shaking motion (160 strokes min^{-1}) was applied in the water bath for 20 min to

ensure that the glass balls were crushed effectively. After removing the centrifuge tube, a volume of 100 μL of the dispersion was collected and immediately vortexed with 1.5 mL of ethanol 75%(v/v) in order to stop the hydrolysis and obtain the *RDS* fraction (G_{20}). After sampling, the centrifuge tube was returned to the shaking water bath for a further 100 min. Thus, after 120 min of incubation, another 100 μL of dispersion was collected and vortexed with ethanol to obtain the G_{120} fraction (*SDS*). The total glucose content was estimated by spectrophotometry at 510 nm using both G_{20} and G_{120} fractions after the reaction with glucose oxidase and peroxidase. The data are computed in g/100 g starch db excluding free glucose. We non-dimensionalize each of the digestibility fractions in turn. First, we denote the dimensionless quality of the rapidly digestible starch fraction by *RDS**, and define it as follows:

$$RDS^* = \frac{RDS - RDS_0}{RDS_1 - RDS_0} \tag{4}$$

Next, we denote the dimensionless quality of the resistant starch fraction as *RS**, and define it as follows:

$$RS^* = \frac{RS - RS_0}{RS_1 - RS_0} \tag{5}$$

For Eqs. (4) and (5), the initial condition ($\alpha = 0$), $RDS = RDS_0$ or $RS = RS_0$ is another way of expressing the dimensionless equations $RDS^* = 0$ or $RS^* = 0$. For $\alpha = 1$, the starch digestibility fractions reach $RDS = RDS_1$ and $RS = RS_1$, and the corresponding dimensionless equations are $RDS^* = 1$ and $RS^* = 1$. Normalizing data to dimensionless digestibility fractions may be particularly helpful as it makes it possible to run multiple transformations (here *RDS*, *RS*) with different absolute amounts (RDS_0, RS_0, RDS_1, RS_1) that can be compared on the same plot. Dimensionless data (Y^*) were also adjusted as Y^* *vs* the degree of starch gelatinization, α, as follows

$$Y^* = \frac{1 - \exp(-a_Y \alpha)}{1 - \exp(-a_Y)} \tag{6}$$

where $Y^* = RDS^*$ or RS* and a_Y is a constant parameter for the Y response. The Eq. (6) is consistent with the definition of the dimensionless fraction: $Y^* = 0$ when $\alpha = 0$ and $Y^* = 1$ when $\alpha = 1$.

2.2.10. Estimating the model parameters

The shape parameter β, scale parameter γ and location parameter θ were estimated using non-linear regression (TableCurve2D® V2.03, SPSS Inc., Chicago, USA) at each water content from the relationship Eq. (2), between α and (T, X_1). For Eq. (6), the values of a_y, were derived by regression (TableCurve2D® V2.03, SPSS Inc., Chicago, USA) between 55 °C and 120 °C. Therefore, uncertainties in identified parameter values (β, θ and a_α), noted as u_β, u_θ and u_{a_α}, respectively, were estimated to have a 95% confidence interval.

2.2.11. Statistical methods

Data obtained on the shape and location parameters were subjected to a preliminary analysis of variance (Statistica® V7.0, Statsoft Inc., Tulsa, USA). The treatments were compared using the *t*-test. The joint effect of the uncertainty (at a 95% confidence interval) of three parameters (β, θ and a_α), provided an uncertainty u_α (at a 95% confidence interval) in terms of the degree of plantain starch gelatinization as a function of temperature and water content, α (Eq. (2a) with Eq. (3)) by:

$$\frac{u_\alpha}{\alpha} = \left(1 - \frac{1}{\alpha}\right) \beta^2 \ln(\alpha - 1) \left\{ \left(\frac{u_{a_\alpha}}{a_\alpha}\right)^2 + \left(\frac{u_\theta}{T - \theta}\right)^2 + \left[\frac{\ln(\ln(\alpha - 1))}{\beta}\right]^2 \left(\frac{u_\beta}{\beta}\right)^2 \right\}^{1/2} \tag{7}$$

In the uncertainty expression, the variables β, θ and a_α were assumed to be independent (in which case the covariance was zero).

The analysis of variance (ANOVA) and mean comparison (Tukey *post hoc* test) were performed to compare estimated *RDS** and *RS** fractions at a confidence level of 95% and 99% using Statistica v.10 software package (StatSoft Inc., Tulsa, Oklahoma). The relationships between the starch gelatinization variable (α) and hydrothermal conditions (T, X_1) in each dimensionless response type (*RDS** and *RS**) were evaluated using a statistical Pearson product-moment correlation coefficient.

3. Results and discussion

3.1. Material characterization

Total starch content and amylose content of the Dominico Harton landrace were estimated to be about 88.3 ± 1.1% (*i.e.* kg starch per 100 kg flour on dry basis) and 21.9 ± 1.5% (*i.e.* kg amylose per 100 kg starch on dry basis), respectively. These results are consistent with some other studies (Dufour et al., 2009; Gibert et al., 2009). The latter reported a higher amylose content in true plantain, such as Dominico Harton, than in dessert banana genotypes with about 23.4 ± 1.1% and 17.4 ± 1.9%, respectively. Dominico Harton starch exhibited an average granule diameter of 27.8 μm with a broad monomodal distribution (14.6–56.2 μm), consistent to previous observations (Eggleston, Swennen, & Akoni, 1992; Hernández-Jaimes, Bello-Pérez, Vernon-Carter, & Alvarez-Ramirez, 2013). Starch extracted from Dominico Harton exhibited a crystalline order of 35% and a mix population of starch granules with 60% of B pattern and 40% of A pattern, which was consistent with other research findings on banana starches (Zhang & Hamaker, 2012). The rate and extent of starch hydrolysis are two of the factors that may also be influenced by structural features, such as crystallinity and crystalline type (Englyst et al., 1992; Faisant et al., 1995; Jane et al., 1999).

With a flour specific gravity estimated to be about 1580.0 ± 0.1 kg m^{-3}, the water volume fraction (ν_1) in the plantain flour was estimated to range from 0.67 to 0.75 m^3 m^{-3} for 1.4 and 2.0 kg kg^{-1} db, respectively.

3.2. Thermal transitions by DSC

Fig. 1 shows normalized and baseline subtracted DSC thermograms for Dominico Harton flour–water mixtures with different water contents (X_1). The onset, peak and end temperatures for the gelatinization transition were 69.7 ± 0.3 °C, 73.7 ± 0.4 °C and 79.7 ± 0.8 °C, respectively. We checked that these three temperatures were independent of water content according to Cruz-Orea, Pitsi, Jamée, and Thoen (2002). The whole enthalpy change (ΔH_e) was slightly water content dependent. For example, ΔH_e were 19.0 ± 1.1 kJ kg^{-1} db and 20.5 ± 0.9 kJ kg^{-1} db, for water content 1.4 and 2.0 kg kg^{-1} db, respectively. The biphasic endothermic transition described by Donovan (1979) in the presence of limited amounts of water was observed, and corresponds to the limited water content condition ($\nu_1 < 0.75$) later reported by Colonna and Mercier (1985). The first endotherm labelled as "G endotherm" was then followed by a small shoulder corresponding to the starch fusion peak labelled as "M1" by Donovan and Mapes (1980). With increasing water content, the intensity of the G endotherm

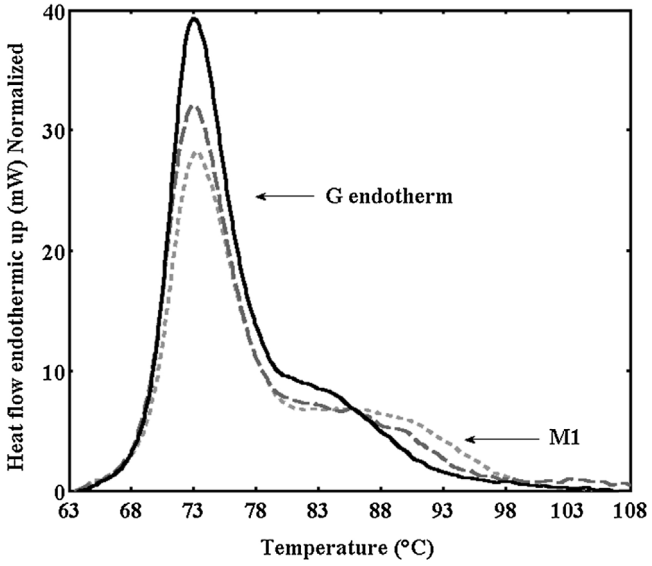

Fig. 1. Endotherms recorded for Dominico Harton plantain flour mixture with different water contents: 1.4 kg kg^{-1} dry basis (▬ ▬), 1.5 kg kg^{-1} dry basis (▬ ▬), 2.0 kg kg^{-1} dry basis (▬▬).

increased whereas its temperature was stable. In the meantime, the M1 endotherm intensity and transition temperature gradually decreased with an increase in X_1. This progressive shift was described as the variation of the melting point of starch crystallites (Donovan, 1979), identified as the melting temperature by (Biliaderis et al., 1980) and later reported by Colonna and Mercier (1985) as the cooperative processes that occur during crystallite melting and starch swelling at high water content. DSC thermograms are shown in Fig. 2 for a Dominico Harton flour–water mixture at 1.4 kg of water per kg of dried plantain flour. A partial heat treatment causes an increase in the onset temperature, the peak temperature and the end temperature and decreases the intensity of the G and M1 endotherms. A partial heat treatment at 75 °C leads to the disappearance of the G endotherm; beyond 90 °C, both endotherms had disappeared. These observations are in accordance with those previously observed for lower water content ranges (Biliaderis et al., 1980; Briffaz et al., 2013; Donovan, 1979).

A small shift of the baseline was observed at the beginning of the thermal transition. It could correspond to the glass transition (T_g) and induced an overestimation of ΔH_e. The location of the temperature of the effective T_g was used for computing corresponding ΔH_e. T_g was identified below the onset of gelatinization and ranges between 56 °C and 60 °C. No significant modification of T_g was observed in the 1.4 and 2.0 kg kg^{-1} db flour range (data not shown). In such high water content systems, increasing water content of the starch mixture should decrease T_g (Slade & Levine, 1991). The lack of variation of T_g in our case is probably due to the narrow water content range used in our study.

ΔH_e was thus calculated considering the thermal event dedicated to the plantain starch non-equilibrium melting transition. The computation of the degree of starch gelatinization α at various water contents and temperatures led us to consider variations of enthalpies for gelatinization according to Eq. (1) while taking into account the sum of all thermal transitions G and M1. The cumulative Weibull model fits the experimental α values well on the whole X_1 domain for 1.4–2.0 kg kg^{-1} db (Fig. 3A). The experimental values obtained with the DSC were adjusted to a 3-parameter Weibull cumulative model using Eq. (2). In a preliminary analysis (data not shown), the 3-parameters β, θ and γ were identified for four different water contents. The statistical analysis shows that the β and θ values do not significantly differ from one another

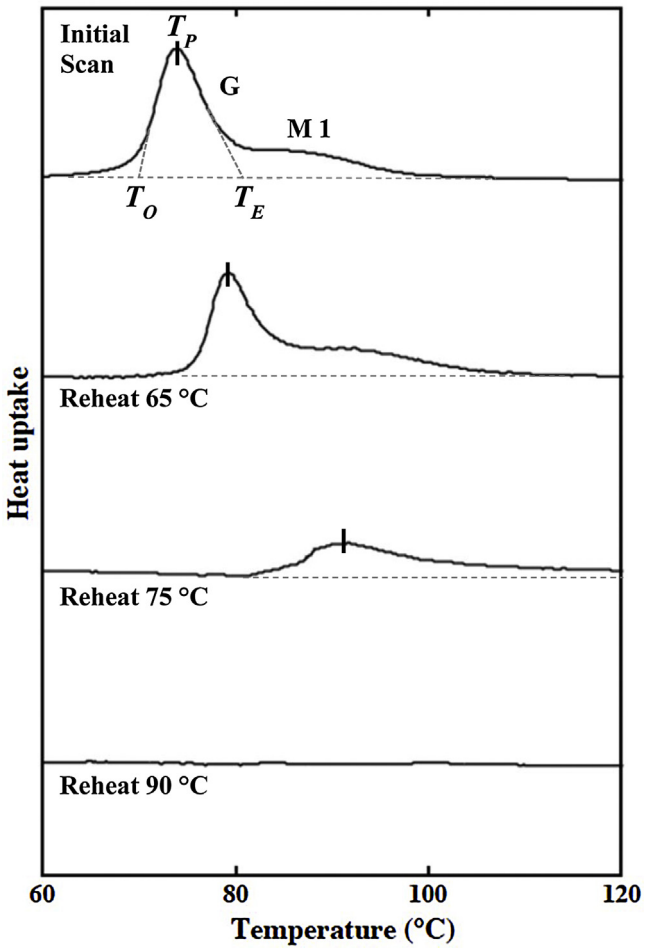

Fig. 2. Native endotherms and endotherms after reheating registered for Dominico Harton plantain flour with a water content of 1.4 kg kg^{-1} dry basis.

between 1.4 and 2.0 kg kg^{-1} db. θ is the location parameter of the distribution and corresponds to the "start transition temperature". It is independent of X_1 according to previous research (Baks, Ngene, van Soest, Janssen, & Boom, 2007; Donovan, 1979; Garcia et al., 1996). However, the γ-parameter is strongly dependent on the water content. Thus, the water dependence on γ is assumed to be inversely proportional to water content X_1 (Eq. (3)). This empirical equation was chosen for its simplicity (just 1 parameter and 4 different water contents) and its good data fitting ($R^2 = 0.80$). The parameter values identified by non-linear regression are $\beta = 1.3 \pm 0.1$, $\theta = 59.6.5$ °C and $a_\alpha = 19.1 \pm 1.0$. In the 55–120 °C range and 1.4 and 2.0 kg kg^{-1} db range, the determination coefficient values ($R^2 = 0.99$) show that the Weibull model provides quite an accurate reflection of the state diagram for plantain flour (Fig. 3A). Moreover, with the degree of starch gelatinization α determined for the 3 parameters (β, θ and a_α) a close fit between the experimental and simulated degree of starch gelatinization was obtained with a root-mean-square error of starch gelatinization equal to 3%. θ value is located close to the upper limit of the T_g range (56 °C $\leq T_g \leq$ 60 °C).

Within a limited water system, Fukuoka, Ohta, and Watanabe (2002) calculated the terminal extent of starch gelatinization (*TEG*), equivalent to α, from an empirical equation on temperature and water content. However, this model has a limited validity range between 0.54 and 1.50 kg kg^{-1} db and it does not take into account the endothermic melting of starch crystallites that is predominant at low water content. Some other authors later considered the Flory–Huggins free volume theory for predicting the temperature

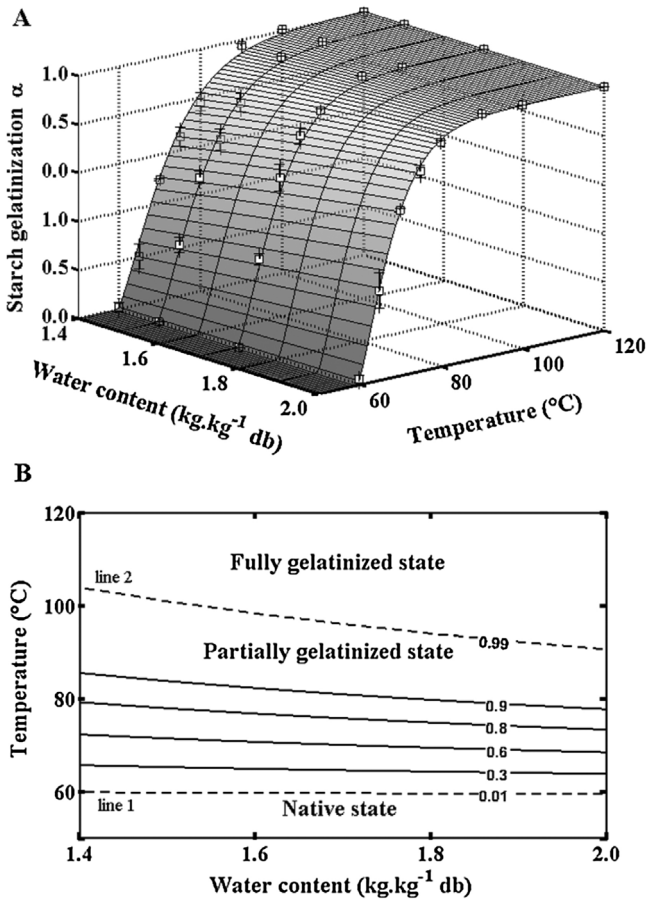

Fig. 3. Modelling phase diagram of plantain flour–water mixtures (starch conversion α *vs* treatment temperature and water content in db). From the change of starch gelatinization α, the physically modified states of heated plantain flour–water mixtures were classified into three states: native state (below line 1: $T < 59.6\,^{\circ}C$), partially gelatinized state (area between line 1 and line 2: $0 < \alpha < 1$) and fully gelatinized state (beyond line 2: $\alpha = 0.99$).

of starch gelatinization (onset of gelatinization) and end of melting (Baks et al., 2007; van der Sman & Meinders, 2011). However, the authors successfully identified different parameters, such as the heat of fusion per repeating unit, the melting point of the pure polymer and Flory–Huggins polymer–diluent interaction parameter. However, they failed to build a model taking into account the end of melting at a water activity above 0.8. In the model for starch thermal transitions developed by Briffaz et al. (2013) for a rice flour/water system, data for a double sigmoid fitting α was expressed over temperature for each water content. This double sigmoid fitting requires 5 parameters for each water content and an additional 10 parameters to take water content into account. This prohibitive number of parameters (15) was justified by the breadth of water content (dry rice to cooking rice). Moreover, the second sigmoid makes it possible to integrate the melting of the amylose-lipid complex. In our specific case, no second sigmoid was necessary. Although the lipid content in unripe green banana flour is in the 0.33–0.82% db range (Mota, Lajolo, Cordenunsi, & Ciacco, 2000), no melting of the amylose-lipid complex was observed in our study. Therefore, the degree of starch gelatinization α was expressed as a function of T, and X_1 with just 3 parameters. In addition to the experimental data and Weibull fitting model in Fig. 3A, the phase diagram was constructed to evaluate the extent of plantain starch gelatinization over temperature and water content (Fig. 3B). For a given temperature and especially for the lowest temperatures of the model (below 70 °C

Table 1
Pearson's correlation coefficients between the experimental dimensionless rapidly digestible starch fraction (RDS^*) or dimensionless resistant starch fraction (RS^*) and starch gelatinization (α) and hydrothermal condition: temperature (T) and water content (X_1).

Variables	RDS^*	RS^*	α	T (°C)	X_1 (kg kg^{-1} db)
RDS^*	1.00		–	–	–
α	0.95***		1.00	–	–
T (°C)	0.69***		0.82***	1.00	–
X_1 (db)	0.02		−0.01	−0.01	1.00
RS^*		1.00	–	–	–
α		0.86***	1.00	–	–
T (°C)		0.59***	0.83***	1.00	–
X_1 (kg kg^{-1} db)		0.10	0.08	0.01	1.00

Statistical probability of correlation coefficients: no superscript, $P > 0.05$.
*Coefficient significant at $P < 0.05$.
**Coefficient significant at $P < 0.01$.
*** Coefficient significant at $P < 0.001$.

approximately), we observe an almost horizontal iso-response in terms of the extent of gelatinization of the plantain starch over water content. As expected, below the θ-temperature, whatever the water content, no gelatinization occurred. As soon as the temperature rises, the iso-responses for the extent of starch gelatinization become more vertical, and there is a potential reduction in the contribution of water to the phenomenon. It suggests that the extent of starch gelatinization is very dependent on temperature in non-limiting water conditions, as was the case in our study. The result was confirmed by a strong correlation between the extent of starch gelatinization and temperature on experimental data (Table 1). The phase diagram could then be used to predict the degree of starch gelatinization according to the processing conditions, *i.e.* water content (1.4–2.0 kg kg^{-1} db) and temperature (55–120 °C). Three states can be distinguished: native state (below iso-response line 1 for $T < 59.6 \pm 0.5\,^{\circ}C$), partially gelatinized state (area between iso-responses $0 \leq \alpha \leq 1$) and fully gelatinized state (above line 2, $\alpha = 0.99$). For the same water content range, the overall shape of the plantain flour state diagram is similar to the rice flour state diagram (Briffaz et al., 2013) and the wheat flour state diagram (Kaletunç & Breslauer, 1996). To start starch gelatinization, the plantain flour/water system requires a higher temperature (+3.6 °C) than rice flour (Briffaz et al., 2013) and a lower temperature (−4.4 °C) than for wheat flour (Kaletunç & Breslauer, 1996). For the same water content (1.4 kg kg^{-1} db), the complete gelatinization ($\alpha = 1$) for wheat–flour/water, rice–flour/water and plantain flour/water systems, requires an increase in temperature from the start of starch gelatinization of approximately +6 °C, +37 °C and +44 °C, respectively (Briffaz et al., 2013; Kaletunç & Breslauer, 1996).

3.3. Degree of starch gelatinization in the test cell

The extent of thermal gelatinization in both the DSC and the cooking device were evaluated and plotted (Fig. 4) for both 1.4 and 2.0 kg kg^{-1} db conditions. Some discrepancies in the extent of starch gelatinization were observed between both cooking apparatuses in the 55–70 °C range. Some slight differences in the heat temperature inside the devices were indeed observed using a calibrated temperature control sensor (data not shown). We observed a slightly lower heating rate within the test cell. This was probably due to its higher volume capacity (10 mL *vs* 60 μL). In addition, for the DSC, the temperature inside the can is corrected by the calibration procedure, which takes into account the inertia of the system. Nevertheless, no significant difference was observed between $\alpha(T)$ for either the test cell or the DSC device above a

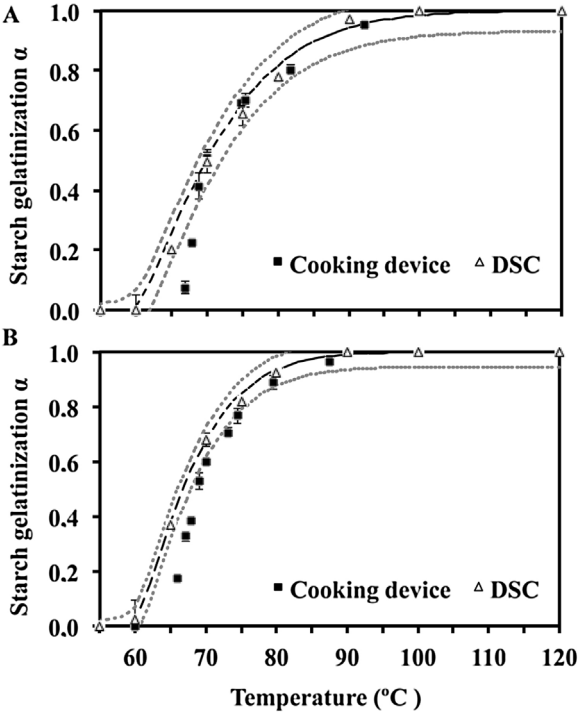

Fig. 4. Comparison between a cooking device and DSC (starch gelatinization α *vs* treatment temperature) for both water contents on dry basis: 1.4 kg kg^{-1} (A) and 2.0 kg kg^{-1} (B).

starch gelatinization of about 0.6. Thus, we were able to validate the use of the test cell to simulate the DSC cooking process.

3.4. Relation between the degree of starch gelatinization and digestibility in vitro

As expected (Chung, Lim, & Lim, 2006), the *RDS* increased and the *RS* decreased when the extent of thermal gelatinization increased. *RDS* values for native flour (Table 2) were consistent with those (11.0 ± 0.7%) reported for raw banana flour by Zhang and Hamaker (2012). A plantain flour–water mixture cooked at 100 °C or above also exhibited slightly higher *RDS* values (90.5 ± 3.7% at 2.0 kg kg^{-1} db) than those reported by previous authors (72.8 ± 4.2%). The difference observed between our investigation and those carried out by Zhang and Hamaker (2012) could be partially attributed to the use of different varieties (unspecified banana *vs* plantain cultivar). As far as the resistant starch fraction is concerned, the investigation carried out by Zhang and Hamaker (2012) reported 83.4% db in raw banana flour. However, in our study no significant difference was observed for native starch, irrespective of the water content (with 84.3 ± 3.8% and 81.2 ± 1.0% db), although for full-gelatinized samples, a slight remaining *RS* fraction was observed at 1.4 kg kg^{-1} db whereas no remaining *RS* fraction was observed at 2.0 kg kg^{-1} db (0.0 ± 0.1% db). The normalized *RDS** and *RS** over the extent of starch gelatinization are plotted in Fig. 5. The model obtained for both *RDS** and *RS** fitted experimental data well for both water conditions. In addition, Table 2 reported the identified a_y parameters for both dimensionless fittings of *RDS** and *RS**, with a reliable RMSE and an indicative R^2, around 6% and above 0.96, respectively. No significant differences between experimental *RDS* over water were observed at either $\alpha = 0$ or $\alpha = 1$, with approximately 11% db and 87–90% db, respectively.

Fig. 5 clearly illustrates the impact of the extent of gelatinization on the dimensionless digestibility of the starch fractions (*RDS** and *RS**). A continuous increase of the normalized *RDS** fraction was

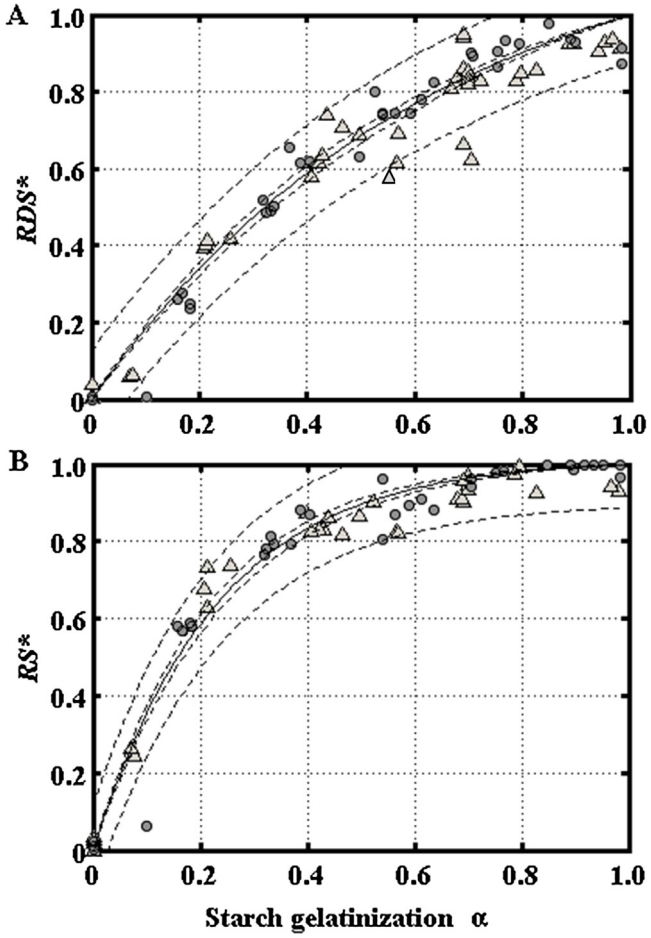

Fig. 5. Dimensionless rapidly digestible starch fraction (*RDS**) and resistant starch fraction (*RS**) of plantain flour as a function of the degree of plantain starch gelatinization (α). Experimental data at different water contents 1.4 kg kg^{-1} db (▲) and 2.0 kg kg^{-1} db (●) and predicted curves: dashed (-·-) line represent the confidence interval and (–) the predicted interval ($P = 0.05$).

observed along the starch gelatinization rate (Fig. 5A). *RDS** was positively correlated to α and to a lesser extent to temperature as shown in Table 1. While starch gelatinization can explain 95% of the variation of *RDS**, temperature accounted for 69% of the variation of *RDS**. The same results were observed for *RS**, however *RS* content decreases with extent of starch gelatinization, but as far as *RS** concerned, an increase of *RS** is observed on Fig. 5B with starch gelatinization. The *RS** values are very dependent on starch gelatinization in the 0.0–0.4α range (Fig. 5B). Holm et al. (1988) reported earlier that *RS* varies proportionally with the degree of gelatinization for wheat starch. The 0.0–0.4α range corresponded to the highest rate of production of *SDS* (data not shown). Contrary to the decrease of *SDS* with the rise of *RDS*, a slight modification of *RS* is usually observed at an advanced extent of gelatinization (Miao et al., 2010). Thus, a slight variation of the *RS** was observed for an advanced rate of starch gelatinization. Accordingly, the latest stage for starch gelatinization corresponded to the minimal production of *SDS* and *RS*. Starch gelatinization and temperature accounted for 86% and 59% of the variation of the *RS* fraction (Table 2), respectively. The dependence of starch gelatinization on temperature illustrated by the phase diagram (Fig. 3) was confirmed by the strong correlation observed between α and T for *RDS** and *RS** as shown in Table 1.

Based on other resources, Chung et al. (2006) and Miao et al. (2010) have already reported that thermal treatment has a considerable impact on the extent of rice or maize gelatinization

Table 2
Parameters a_Y for the fit of dimensionless $Y^* = (Y - Y_0)/(Y_1 - Y_0)$ response $Y^* = [1 - \exp(-a_Y\alpha)]/[1 - \exp(-a_Y)]$ as a function of starch gelatinization (α) at different water contents (X_1) with $Y^* = RDS^*$ the dimensionless rapidly digestible starch fraction and $Y^* = RS^*$ the dimensionless resistant starch fraction.

Y^*	X_1 (kg kg^{-1} db)	Y_α value (kg/100 kg dry starch)		a_Y	R^2	RMSE
		$\alpha = 0$	$\alpha = 1$			
*RDS**	1.4	11.0 ± 0.7a	86.9 ± 8.8b	1.56 ± 0.2	0.96	0.06
	2.0	11.2 ± 0.4a	90.5 ± 3.7b			
*RS**	1.4	84.3 ± 3.8c	4.3 ± 2.8d	4.30 ± 0.3	0.97	0.06
	2.0	81.2 ± 1.0c	0.0 ± 0.1e			

Value ± confidence interval ($P = 0.05$).
RMSE: Root mean square error of Y^* between experimental and simulated data.
In the column Y_0 and Y_1 values with same letters are not significantly different ($P < 0.05$).

and digestibility. Parada and Aguilera (2009) noted that 100% gelatinized potato starch corresponds to 100% digestible starch. For plantain flour, it was observed that 100% of starch gelatinization did not correspond to a 100% level of digestibility. The lower digestibility of gelatinized plantain starch can be partially explained by the amylose content. Amylose is normally associated with the less digestible properties of cooked starches. In addition, amylopectin structures in banana plantain starch have shown differences to support the theory that it has less good *in vitro* digestion properties. The hypothesis was recently put forward suggesting that the high proportion of the long chains of banana amylopectin reduce susceptibility to enzyme attack on cooling after cooking (Zhang & Hamaker, 2012). Indeed, Zhang and Hamaker suggested that the complexes formed during starch retrogradation that were previously considered to be a retrograde resistant starch type III could potentially make a contribution (Englyst et al., 1992).

4. Conclusion

Here we have modelled starch thermal transitions. A 3-parameter Weibull model was fitted with DSC data for any water content (X_1). For each water content, the degree of starch gelatinization α was expressed as a function of the temperature T. The combined effects of temperature and water content on the *in vitro* digestibility properties can be summarized by starch conversion (α) irrespective of the heat-treatment history. So, two empirical models were proposed to predict *RDS* and *RS* as a function of starch gelatinization. In the water content range of banana plantain (raw to cooked), the temperature is the main factor that influences starch conversion and digestibility. These models (state diagram, *RDS* and *RS* response) will now be integrated in a heat and mass transfer model with the aim of optimizing the plantain cooking process.

Acknowledgements

Dr. Agnès Rolland-Sabaté and Dr. Brunot Pontoire INRA for the DRX measurements. COLFUTURO (Colombian Organization) and Bourse EIFFEL (French – Ministry of International Relations) institutions for funding this work.

References

Bahado-Singh, P. S., Wheatley, A. O., Ahmad, M. H., Morrison, E. Y. S. A., & Asemota, H. N. (2006). Food processing methods influence the glycaemic indices of some commonly eaten West Indian carbohydrate-rich foods. *British Journal of Nutrition*, *96*(3), 476–481.

Baks, T., Ngene, I. S., van Soest, J. J. G., Janssen, A. E. M., & Boom, R. M. (2007). Comparison of methods to determine the degree of gelatinization for both high and low starch concentrations. *Carbohydrate Polymers*, *67*(4), 481–490. http://dx.doi.org/10.1016/j.carbpol.2006.06.016

Bello-Perez, L. A., Agama-Acevedo, E., Gibert, O., & Dufour, D. (2012). Banana. In E. M. Siddiq (Ed.), *Tropical and Subtropical Fruits* (pp. 135–157). Wiley-Blackwell. Recovery: http://onlinelibrary.wiley.com/doi/10.1002/9781118324097.ch8/summary

Biliaderis, C. G., Maurice, T. J., & Vose, J. R. (1980). Starch gelatinization phenomena studied by differential scanning calorimetry. *Journal of Food Science*, *45*(6), 1669–1674. http://dx.doi.org/10.1111/j. 1365-2621.1980.tb07586.x

Briffaz, A., Bohuon, P., Méot, J.-M., Dornier, M., & Mestres, C. (2014). Modelling of water transport and swelling associated with starch gelatinization during rice cooking. *Journal of Food Engineering*, *121*, 143–151. http://dx.doi.org/10.1016/j.jfoodeng.2013.06.013

Briffaz, A., Bohuon, P., Méot, J.-M., Pons, B., Matencio, F., Dornier, M., & Mestres, C. (2014). Modelling of brown rice and limited-water cooking modes and its potential use for texture prediction. *Journal of Food Engineering*, *141*, 99–106. http://dx.doi.org/10.1016/j.jfoodeng.2014.05.008

Briffaz, A., Mestres, C., Matencio, F., Pons, B., & Dornier, M. (2013). Modelling starch phase transitions and water uptake of rice kernels during cooking. *Journal of Cereal Science*, *58*(3), 387–392. http://dx.doi.org/10.1016/j.jcs.2013.08.001

Chung, H.-J., Lim, H. S., & Lim, S.-T. (2006). Effect of partial gelatinization and retrogradation on the enzymatic digestion of waxy rice starch. *Journal of Cereal Science*, *43*(3), 353–359. http://dx.doi.org/10.1016/j.jcs.2005.12.001

Colonna, P., & Mercier, C. (1985). Gelatinization and melting of maize and pea starches with normal and high-amylose genotypes. *Phytochemistry*, *24*(8), 1667–1674. http://dx.doi.org/10.1016/S0031-9422(00)82532-7

Cruz-Orea, A., Pitsi, G., Jamée, P., & Thoen, J. (2002). Phase transitions in the starch–water system studied by adiabatic scanning calorimetry. *Journal of Agricultural and Food Chemistry*, *50*(6), 1335–1344. http://dx.doi.org/10.1021/jf0110396

Da Mota, R. V., Lajolo, F. M., Cordenunsi, B. R., & Ciacco, C. (2000). Composition and functional properties of banana flour from different varieties. *Starch – Stärke*, *52*(2–3), 63–68. http://dx.doi.org/10.1002/(SICI)1521-379X(200004)52:2/3<63:AID-STAR63>3.0.CO;2-V

Donovan, J. W. (1979). Phase transitions of the starch–water system. *Biopolymers*, *18*(2), 263–275. http://dx.doi.org/10.1002/bip.1979.360180204

Donovan, J. W., & Mapes, C. J. (1980). Multiple phase transitions of starches and nägeli amylodextrins. *Starch – Stärke*, *32*(6), 190–193. http://dx.doi.org/10.1002/star.19800320604

Dufour, D., Gibert, O., Giraldo, A., Sánchez, T., Reynes, M., Pain, J.-P., Gonzalez, A., Fernandez, A., & Diaz, A. (2009). Differentiation between cooking bananas and dessert bananas. 2. Thermal and functional characterization of cultivated Colombian musaceae (*Musa* sp.). *Journal of Agricultural and Food Chemistry*, *57*(17), 7870–7876. http://dx.doi.org/10.1021/jf900235a

Eggleston, G., Swennen, R., & Akoni, S. (1992). Physicochemical studies on starches isolated from plantain cultivars, plantain hybrids and cooking bananas. *Starch – Stärke*, *44*(4), 121–128. http://dx.doi.org/10.1002/star.19920440402

Englyst, H. N., & Cummings, J. H. (1986). Digestion of the carbohydrates of banana (*Musa paradisiaca sapientum*) in the human small intestine. *American Journal of Clinical Nutrition*, *44*(1), 42–50.

Englyst, H. N., Kingman, S. M., & Cummings, J. H. (1992). Classification and measurement of nutritionally important starch fractions. *European Journal of Clinical Nutrition*, *46*(Suppl. 2), S33–S50.

Englyst, H. N., Veenstra, J., & Hudson, G. J. (1996). Measurement of rapidly available glucose (RAG) in plant foods: A potential in vitro predictor of the glycaemic response. *British Journal of Nutrition*, *75*(3), 327–337.

Faisant, N., Buléon, A., Colonna, P., Molis, C., Lartigue, S., Galmiche, J. P., & Champ, M. (1995). Digestion of raw banana starch in the small intestine of healthy humans: Structural features of resistant starch. *British Journal of Nutrition*, *73*(01), 111–123. http://dx.doi.org/10.1079/BJN19950013

FAOSTAT (2013) retrieve from: http://faostat3.fao.org/faostat-gateway/go/to/home/E

Fukuoka, M., Ohta, K., & Watanabe, H. (2002). Determination of the terminal extent of starch gelatinization in a limited water system by DSC. *Journal of Food Engineering*, *53*(1), 39–42. http://dx.doi.org/10.1016/S0260-8774(01)00137-6

Garcia, V., Colonna, P., Lourdin, D., Buleon, A., Bizot, H., & Ollivon, M. (1996). Thermal transitions of cassava starch at intermediate water contents. *Journal of Thermal Analysis*, *47*(5), 1213–1228. http://dx.doi.org/10.1007/BF01992824

Gibert, O., Dufour, D., Giraldo, A., Sánchez, T., Reynes, M., Pain, J. P., Fernandez, A., & Diaz, A. (2009). Differentiation between cooking bananas and dessert bananas. 1. Morphological and compositional characterization of cultivated Colombian musaceae (*Musa* sp.) in relation to consumer preferences. *Journal of Agricultural and Food Chemistry*, *57*(17), 7857–7869. http://dx.doi.org/10.1021/jf901788x

Gibert, O., Giraldo, A., Uclés-Santos, J.-R., Sánchez, T., Fernández, A., Bohuon, P., Reynes, M., Gonzalez, A., Pain, J. P., & Dufour, D. (2010). A kinetic approach to

textural changes of different banana genotypes (*Musa* sp.) cooked in boiling water in relation to starch gelatinization. *Journal of Food Engineering*, *98*(4), 471–479. http://dx.doi.org/10.1016/j.jfoodeng.2010.01.030

Hernández-Jaimes, C., Bello-Pérez, L. A., Vernon-Carter, E. J., & Alvarez-Ramirez, J. (2013). Plantain starch granules morphology, crystallinity, structure transition, and size evolution upon acid hydrolysis. *Carbohydrate Polymers*, *95*(1), 207–213. http://dx.doi.org/10.1016/j.carbpol.2013.03.017

Holm, J., Björck, I., Drews, A., & Asp, N. G. (1986). A rapid method for the analysis of starch. *Starch – Stärke*, *38*(7), 224–226.

Holm, J., Lundquist, I., Björck, I., Eliasson, A. C., & Asp, N. G. (1988). Degree of starch gelatinization, digestion rate of starch in vitro, and metabolic response in rats. *American Journal of Clinical Nutrition*, *47*(6), 1010–1016.

Jane, J., Chen, Y., Lee, L., McPherson, A., Wong, K., Radosavljevic, M, & Kasemsuwan, T. (1999). Effects of amylopectin branch chain length and amylose content on the gelatinization and pasting properties of starch 1. *Cereal Chemistry*, *76*(5), 629–637.

Jiménez, N., Bohuon, P., Lima, J., Dornier, M., Vaillant, F., & Pérez, A. M. (2010). Kinetics of anthocyanin degradation and browning in reconstituted blackberry juice treated at high temperatures (100–180 degrees C). *Journal of Agricultural and Food Chemistry*, *58*(4), 2314–2322. http://dx.doi.org/10.1021/jf902381e

Kaletunç, G., & Breslauer, K. J. (1996). Construction of a wheat–flour state diagram. *Journal of Thermal Analysis*, *47*(5), 1267–1288. http://dx.doi.org/10.1007/BF01992827

Lelièvre, J., & Liu, H. (1994). A review of thermal analysis studies of starch gelatinization. *Thermochimica Acta*, *246*(2), 309–315. http://dx.doi.org/10.1016/0040-6031(94)80098-7

Lescot, T. (2013). World plantain and banana production systems. In A. L. Borges, & L. Lichtemberg (Eds.), *Proceedings of the 20th international meeting ACORBAT: 40 years sharing science and technology, Reunion international ACORBAT 2013* Fortaleza, Brazil, 9–13 September, 2013, (pp. 27–34), 2013-09-09/2013-09-13, http://www.cnpmf.embrapa.br/publicacoes/ACORBAT2013/Paletras_Acorbat2013/3%20SPMundo.pdf

Menezes, E. W., Dan, M. C. T., Cardenette, G. H. L., Goñi, I., Bello-Pérez, L. A., & Lajolo, F. M. (2010). In vitro colonic fermentation and glycemic response of different kinds of unripe banana flour. *Plant Foods for Human Nutrition*, *65*(4), 379–385. http://dx.doi.org/10.1007/s11130-010-0190-4

Mestres, C., Matencio, F., Pons, B., Yajid, M., & Fliedel, G. (1996). A rapid method for the determination of amylose content by using differential-scanning calorimetry. *Starch – Stärke*, *48*(1), 2–6. http://dx.doi.org/10.1002/star.19960480103

Miao, M., Zhang, T., Mu, W., & Jiang, B. (2010). Effect of controlled gelatinization in excess water on digestibility of waxy maize starch. *Food Chemistry*, *119*(1), 41–48. http://dx.doi.org/10.1016/j.foodchem.2009.05.035

Niba, L. L. (2003). Processing effects on susceptibility of starch to digestion in some dietary starch sources. *International Journal of Food Sciences and Nutrition*, *54*(1), 97–109. http://dx.doi.org/10.1080/096374803/000042038

Parada, J., & Aguilera, J. M. (2009). In vitro digestibility and glycemic response of potato starch is related to granule size and degree of gelatinization. *Journal of Food Science*, *74*(1), E34–E38. http://dx.doi.org/10.1111/j.1750-3841.2008.01016.x

Pérez, E., Gibert, O., Rolland-Sabaté, A., Jimenez, Y., Sanchéz, T., Giraldo, A., & Dufour, D. (2011). Physicochemical, functional, and macromolecular properties 2 of waxy yam starches discovered from «Mapuey» 3 (*Dioscorea trifida*) genotypes in the Venezuelan Amazon. *Journal of Agricultural and Food Chemistry*, *59*(1), 263–273. http://dx.doi.org/10.1021/jf100418r

Singh, J., Dartois, A., & Kaur, L. (2010). Starch digestibility in food matrix: A review. *Trends in Food Science & Technology*, *21*(4), 168–180. http://dx.doi.org/10.1016/j.tifs.2009.12.001

Slade, L., & Levine, H. (1988). Non-equilibrium melting of native granular starch: Part I. Temperature location of the glass transition associated with gelatinization of A-type cereal starches. *Carbohydrate Polymers*, *8*(3), 183–208. http://dx.doi.org/10.1016/0144-8617(88)90002-1

Slade, L., & Levine, H. (1991). A food polymer science approach to structure-property relationships in aqueous food systems: non-equilibrium behavior of carbohydrate–water systems. *Advances in Experimental Medicine and Biology*, *302*, 29–101.

Tribess, T. B., Hernández-Uribe, J. P., Méndez-Montealvo, M. G. C., Menezes, E. W., Bello-Perez, L. A., & Tadini, C. C. (2009). Thermal properties and resistant starch content of green banana flour (*Musa cavendishii*) produced at different drying conditions. *LWT – Food Science and Technology*, *42*(5), 1022–1025. http://dx.doi.org/10.1016/j.lwt.2008.12.017

Van Boekel, M. A. J. S. (2002). On the use of the Weibull model to describe thermal inactivation of microbial vegetative cells. *International Journal of Food Microbiology*, *74*(1–2), 139–159. http://dx.doi.org/10.1016/S0168-1605(01)00742-5

van der Sman, R. G. M., & Meinders, M. B. J. (2011). Prediction of the state diagram of starch water mixtures using the Flory–Huggins free volume theory. *Soft Matter*, *7*(2), 429. http://dx.doi.org/10.1039/c0sm00280a

Wang, S., & Copeland, L. (2013). Molecular disassembly of starch granules during gelatinization and its effect on starch digestibility: A review. *Food & Function*, *4*(11), 1564–1580. http://dx.doi.org/10.1039/c3fo60258c

Zhang, P., & Hamaker, B. R. (2012). Banana starch structure and digestibility. *Carbohydrate Polymers*, *87*(2), 1552–1558. http://dx.doi.org/10.1016/j.carbpol.2011.09.053